Materials Letters 94 (2013) 193–196

Contents lists available at SciVerse ScienceDirect

Materials Letters

journal homepage: www.elsevier.com/locate/matlet

Corrosion performance and metal ion release of amorphous and nanocrystalline Fe-based alloys under simulated body fluid conditions

H. Zohdi [a], M. Bozorg [a], R. Arabi Jeshvaghani [a], H.R. Shahverdi [a,*], S.M.M. Hadavi [b]

[a] Materials Engineering Department, Tarbiat Modares University, P.O. Box 14115–143, Tehran, Iran
[b] School of Materials Science and Engineering, MA University of Technology, P.O. Box 16765–3197, Tehran, Iran

ARTICLE INFO

Article history:
Received 30 October 2012
Accepted 14 December 2012
Available online 25 December 2012

Keywords:
Amorphous materials
Nanocrystalline structure
Corrosion
ICP

ABSTRACT

The corrosion performance of $Fe_{55-x}Cr_{18}Mo_7B_{16}C_4Nb_x$ ($x=0$ and 3 at%) amorphous and nanocrystalline ribbons in Ringer and 0.9% NaCl+HCl solutions open to air at 37 °C, was investigated by electrochemical polarization analysis, aiming to estimate the feasibility of alloys as potential biomaterials. It was indicated that the both $Fe_{52}Cr_{18}Mo_7B_{16}C_4Nb_3$ amorphous and nanocrystalline ribbons have higher corrosion resistance value than that of 316L stainless steel. Besides, the results showed that the amorphous ribbons have larger polarization resistance value than that of nanocrystalline alloys under the same condition. Interestingly, the results of the inductively coupled plasma apparatus showed that all the samples do not release any significant ions into the Ringer's solution, while there are very few ions releasing into the aqueous 0.9% NaCl+HCl solution for amorphous alloys compared to nanocrystalline alloys and 316L stainless steel.

1. Introduction

Biomedical materials play an important role in manufacturing a variety of prosthetic devices in a modern world. The first requirement for any material to be placed in the human body is that it should be biocompatible and not cause any adverse reaction [1]. Although conventional crystalline materials such as Ti–6Al–4V and 316L SS are considered as better materials for implanted parts, reports have demonstrated that these materials cause some problems in the human body [1,2]. Metal ions released from metallic biomaterials in the body may cause harmful effects on human health. Since the release of metal ions depends on electrochemical rule, many efforts were made for electrochemical analyses of the materials to investigate the metal ion release [3].

Glassy (Amorphous) alloys are relative newcomers in the field of biomaterials but they exhibit an excellent combination of properties and processing capabilities desired for versatile implant applications [4]. Although rapid solidification methods for processing amorphous alloys are well recognized, the need for simultaneous mold filling and rapid cooling rate restricts the range of geometries that can be formed [4,5]. These processing difficulties in combination with low tensile ductility and toughness limit the applications of bulk metallic glasses (BMG). Therefore, metallic glasses (MG) will be more attractive for wear/corrosion resistant coatings on the crystalline substrates used as biomaterials [6,7]. Since the amorphous phase is not thermodynamically stable phase, the amorphous phase transforms into stable crystalline phases or nanosize crystals during thermal treatment, materials processing or in service resulting [8]. So, the biocompatibility properties of nanocrystalline (annealed) alloys should be considered as well as metallic glasses.

In general, reports prove the high corrosion resistance of metallic glasses in various environments. However, limited work has been performed to characterize the biocompatibility of these materials [9]. Among many types of metallic glasses, Fe-based glasses are known to be suitable choices for biocompatible applications owing to their composition, high strength, high hardness, excellent corrosion, wear resistance or a combination of these. Besides, the main element Fe is relatively cheap and is readily available. However, there are few reports on the corrosion properties of Fe-based amorphous alloys in the simulated body fluids [2,10,11]. But, there is no report to compare the corrosion behavior of amorphous with nanocrystalline Fe-based alloys in Ringer and 0.9% NaCl+HCl solutions.

The plan of this research is to compare the corrosion behavior and metal ion release of $Fe_{55-x}Cr_{18}Mo_7B_{16}C_4Nb_x$ ($x=0$ and 3 at%) metallic glasses with these of their nanocrystalline counterpart and the 316L SS. The effects of annealing process on the electrochemical analyses of the materials are also considered.

2. Material and methods

$Fe_{55-x}Cr_{18}Mo_7B_{16}C_4Nb_x$ ($x=0$ and 3 at%) amorphous ribbons were produced by melt spinning technique in an argon atmosphere. The obtained ribbons having no noticeable porosities were 3 mm wide and 60 μm thick, and a density of 7.5–7.7 g/cm^3.

* Corresponding author. Tel./fax: +98 21 82883307.
E-mail address: shahverdi@modares.ac.ir (H.R. Shahverdi).

0167-577X/$ - see front matter © 2012 Elsevier B.V. All rights reserved.
http://dx.doi.org/10.1016/j.matlet.2012.12.051

The nanocrystalline alloys with the same composition were obtained from metallic glasses under high vacuum in the furnace above the first crystallization temperature (923 K) for 3 h, followed by furnace cooling. It would be noted that the crystallization temperatures were determined by differential scanning calorimetry (DSC) which can be found in our previous paper [11]. The structure of ribbons was verified by X-ray diffraction (XRD) using Cu K_α radiation and transmission electron microscopy (TEM) to identify crystallized phases.

The electrochemical behavior of alloys was considered by potentiodynamic polarization in a three-electrode cell with the use of working electrode, a platinum mesh electrode and a saturated calomel reference electrode (SCE). The electrolytes used in this study were Ringer's solution (pH=6.5) and a aqueous 0.9% NaCl solution with low pH in the acidic range, which was prepared by adding analytical quality HCl to give a solution of pH=2. The corrosion tests were performed on the shiny side (surface roughness of less than 5 nm) of the ribbons, which were not in contact with the cooling wheel in melt spinning process. Potentiodynamic polarization curves were measured by EG&G Princeton Applied Research 273A with a potential sweep rate of 2 mV/s open to air at 37 °C after immersing the samples for 1 h, when the open-circuit potentials became almost steady. The metal ions released from immersion specimens into solutions were determined by using an inductively coupled plasma mass spectrometry (ICP-MS, ThermoElemental X7) after being immersed in the Ringer's solution for 84 days and in 0.9% NaCl+HCl solution for 28 days. The analytical detection limits under these conditions were all below 0.5 μg/L.

3. Results and discussion

Fig. 1 shows the high-resolution TEM images and selected-area electron diffraction patterns (the upper left corner of each micrograph) of amorphous and annealed alloys. Fig. 1(a) and (b) exhibits the TEM images of the amorphous samples with 0 and 3 atomic percentage of Nb, respectively. The maze pattern contrasts and halo diffraction patterns demonstrate the typical of a single amorphous structure. Specifically, no crystalline phase was detected in several parts examined by TEM. The TEM images of annealed $Fe_{55-x}Cr_{18}Mo_7B_{16}C_4Nb_x$ (x=0 and 3 at%) ribbons are also shown in Fig. 1(c) and (d). Crystalline phases are seen clearly in these figures. Generally, it can be inferred from Fig. 1 that the obvious difference in TEM structure before and after annealing process indicates that the as-cast ribbons are fully amorphous nature without any crystalline phase, while the annealed ones reveal homogeneous nanocrystalline structure with an average size of 15 nm. Moreover, the XRD was made to give more detailed information.

Fig. 2 shows the XRD patterns of the amorphous and annealed $Fe_{55-x}Cr_{18}Mo_7B_{16}C_4Nb_x$ (x=0 and 3 at%) alloys. As can be seen clearly, no peak corresponding to crystalline phases is detected for amorphous ribbons and they show the broad diffraction peaks at 2θ range of 40–50, which presents the formation of an amorphous single structure. In contrast, the XRD patterns for the annealed samples show that the main phase crystallized in the structure of the ribbons was α-Fe, while Fe_3B phase was only observed in the annealed $Fe_{52}Cr_{18}Mo_7B_{16}C_4Nb_3$ alloy.

The polarization curves for the amorphous and nanocrystalline Fe-based alloys in the Ringer's solution open to air at 37 °C are presented in Fig. 3(a). For comparison, 316L SS was tested under the same conditions. Compared to the amorphous alloys, the nanocrystalline counterpart alloys show less corrosion potentials (E_{corr}) and higher corrosion current densities (I_{corr}), implying that annealing procedure decreases the corrosion resistance of the Fe-based metallic glasses. Since the crystalline phases (α-Fe and Fe_3B) precipitated in the amorphous matrix, it can be concluded that local galvanic cell effects between amorphous and crystalline phases can decrease the corrosion resistance of nanocrystalline alloys [8,12]. Besides, some metallurgical defects like grain

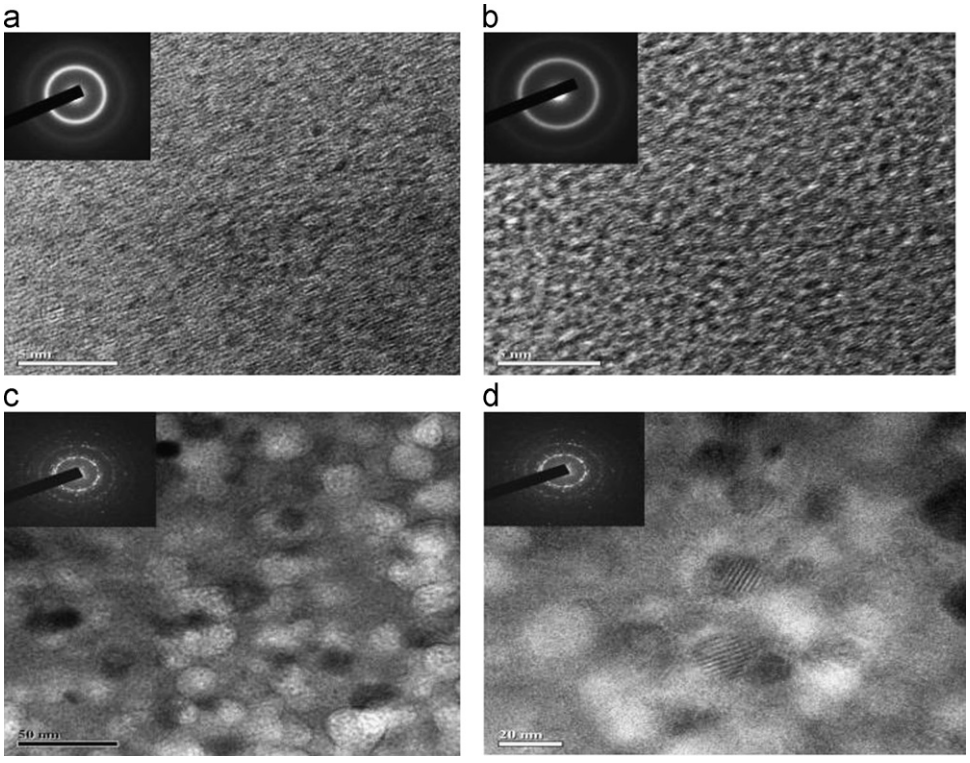

Fig. 1. High-resolution TEM images and selected area electron diffraction patterns of the (a) amorphous $Fe_{55}Cr_{18}Mo_7B_{16}C_4$, (b) amorphous $Fe_{52}Cr_{18}Mo_7B_{16}C_4Nb_3$, (c) nanocrystalline $Fe_{55}Cr_{18}Mo_7B_{16}C_4$ and (d) nanocrystalline $Fe_{52}Cr_{18}Mo_7B_{16}C_4Nb_3$ alloys.